Journal of Tropical Biodiversity and Biotechnology
Volume 08, Issue 03 (2023): jtbb79072
DOI: 10.22146/jtbb.79072

Research Article

Profiling of Single Garlic Extract Microencapsulation: Characterization, Antioxidant Activity, and Release Kinetic

Sri Rahayu Lestari[1]*, Abdul Ghofur[1], Siti Imroatul Maslikah[1], Sunaryono[2], Amalia Nur Rahma[1], Dahniar Nur Aisyah[1], Ikfi Nihayatul Mufidah[1], Nadiya Dini Rifqi[1], Nenes Prastita[1], Dewi Sekar Miasih[1], Alif Rosyidah El Baroroh[1]
1)Departement of Biology, Faculty of Mathemathics and Natural Sciences, Universitas Negeri Malang, Jl. Semarang 5, Malang 65145, Indonesia
2)Departement of Physics, Faculty of Mathemathics and Natural Sciences, Universitas Negeri Malang, Jl. Semarang 5, Malang 65145, Indonesia
* Corresponding author, email: srirahayulestari@um.ac.id

Keywords:
Microencapsulation
Chitosan-alginate
Single garlic extract
Submitted:
10 November 2022
Accepted:
12 June 2023
Published:
23 November 2023
Editor:
Furzani Binti Pa'ee

ABSTRACT
Single garlic is known to have many benefits as an alternative therapy for various types of metabolic syndrome. The bioactive compounds, allicin, and alliin, in garlic are unstable and easily degraded in digestion. Chitosan-alginate microencapsulation is thought to increase stability and protect active compound so its therapeutic effect is more optimal. This study aimed to characterize the microencapsulation chitosan-alginate of single garlic extract (MCA- SGE), as well as to examine the antioxidant activity and kinetic release of MCA-SGE in vitro. The research procedure includes the steps of single garlic extraction, preparation of MCA-SGE, characterization of MCA-SGE (PSA, SEM, and FTIR) as well as biological testing of MCA-SGE through antioxidant activity and kinetic release tests. PSA results showed the mean particle size of MCA-SGE was 439.0 ± 1.9 nm or 0.4 m with a polydispersity index (PDI) value of 0.579 ± 0.046 and a zeta potential value of 15.4 ± 0.3 mV. The SEM results showed that the morphology of MCA-SGE was spherical with a smooth surface and a micrometre size of 0.4 - 0.7 µm. The FTIR results describe a shift in absorption and addition of SGE functional groups after encapsulation. The results of the antioxidant activity test showed the antioxidant activity of MCA -SGE was 65%, while SGE was 55%. The results of the kinetic release showed that more allicin and alliin were released by SGE than MCA-SGE during the 4 -hour kinetic release simulation. MCA-SGE has the potential to be used as a drug delivery system with controlled release.

INTRODUCTION
Single garlic (*Allium sativum*) is a type of garlic with one clove (Lestari et al. 2020). Single garlic has various benefits, such as antioxidant, anti-inflammatory, anticancer, antidiabetic, and anti-obesity (Lestari & Rifa'i 2018; Szychowski et al. 2018; Sasi et al. 2021). Single garlic contains various bioactive compounds in the form of organosulfur and phenolic compounds, including *allicin*, *diallyl sulphide* , *diallyl trisulphide*, *diallyl disulfide*, *ajoene*, and *2-vinyldithiins* (Abdel-Gawad et al. 2018; Shang et al. 2019). *Allicin* and *alliin* are the most dominant organosulfur compounds, but both compounds have the disadvantage of being unstable and easily de-

graded due to pH conditions in the gastrointestinal tract (Bhatwalkar et al. 2021). The weakness of the single garlic bioactive compound can reduce its bioavailability and hinder its potential as a therapeutic agent (Kyriakoudi et al. 2021; Lestari et al. 2021). The solution to overcome the weakness of a single important compound of garlic is to encapsulate the compound in a drug delivery system (Akhter et al. 2022).

Microencapsulation is one of the drug delivery systems to protect bioactive compounds in microcapsules, which are characterised by bioactive compounds coated with encapsulating agents (Alencar et al. 2022). Bioactive compounds will be enclosed between the polymer chain bonds so that a microencapsulated structure is formed on a microparticle scale (Pedroso-Santana & Fleitas-Salazar 2020). The size range of the microparticles is 1 to 1000 m (Lengyel et al. 2019a). The advantages of microencapsulation include protecting bioactive compounds from adverse environmental conditions, controlled release of bioactive compounds, and increasing stability and bio-accessibility (Baltrusch et al. 2022). The polymer in the microencapsulation must be inert to bioactive ingredients, easily soluble, allow controlled release, and compatible with processing conditions (pH/temperature) (Pateiro et al. 2021). Chitosan is a polymer derived from crustacean shells, fungal cell walls, or insect cuticles, while alginate is a polymer extracted from brown algae (Katuwavila et al. 2016). Chitosan and alginate are polyelectrolyte polymers with opposite charges, in addition, when combining alginate with chitosan, it can help stabilise unstable alginates (Katuwavila et al. 2016; Sorasitthiyanukarn et al. 2018). The advantages of chitosan and alginate are that they have biocompatibility, biodegradability, and are non-toxic (Loquercio et al. 2015). Crosslinker $CaCl_2$ acts as a crosslinker in strengthening the bonds between polymers (Tao et al. 2021).

Previous studies have stated that encapsulation can improve the stability of bioactive compounds for the better and increase their solubility (Sorasitthiyanukarn et al. 2018; Machado et al. 2021). According to the research of (Amiri et al. 2021), encapsulation of garlic oil with chitosan can maintain antioxidant content. Research (Natrajan et al. 2015) showed that the results of an in vitro kinetic release study on nano encapsulated turmeric and citronella oil showed an increased bioavailability of the compounds of turmeric oil and citronella oil. Many studies on encapsulation have been carried out, but encapsulation using a single garlic extract as the microencapsulated content of chitosan-alginate has not been reported. This study was conducted with the aim of characterising and testing the effect of chitosan-alginate microencapsulation on antioxidant activity and the results of in vitro kinetic release studies of single garlic extract.

MATERIALS AND METHODS

Materials

The tools used include analytical balance (OHAUS), dry oven, incubator shaker (Stuart), rotary evaporator (IKA RV 10 digital V-C Rotary Evaporator), magnetic stirrer (Thermoline cimarec), centrifuge (Hettich), sonicator (IWAKI), ultra thurrax (IKA-WERKE), pH meter (Hanna), vortex (SIBATA), Scanning Electron Microscopy (SEM) (FEI Quanta FEG 650 type), Malvern Zetasizer (Zetasizer Nano, Version 7.01, Malvern Instruments Ltd.), spectrophotometer (Biochrom Libra S12), IR spectrophotometer (Shimadzu IRSpirit-T), shaker water bath, spatula, stirring rod, beaker glass (Pyrex), micropipette (Thermo), tweezers, syringe (Onemed), volumetric flask (Pyrex), measuring cup (Pyrex), vial, 0.45 µm microfilter (Corning 28 mm Syringe Filter Non-Pyrogenic), stopwatch, and refrigerator (Sharp). The materials used include single garlic from

Sarangan Village, Magetan District, East Java, Indonesia, 70% ethanol (Merck), chitosan (Sigma-Aldrich), alginate (Sigma-Aldrich), Tween-80 (Sigma-Aldrich), acetic acid, 1M NaOH, $CaCl_2$, Phosphate Buffer Saline (PBS), aquabides (Ikapharmindo), selovan bags, sewing thread, gloves, aluminum foil, and plastic wrap.

Methods

Preparation of Single Garlic Extract (SGE)

A total of 1 kg of crushed garlic was macerated in 70% ethanol (1:3) for 3 x 24 hours. The maceration filtrate was evaporated using a rotary evaporator to obtain liquid SGE. SGE is stored at 4°C (Qadariah et al. 2020).

Preparation of MCA-SGE

The nano encapsulated components consisted of: alginate in 0.5% Tween-80 (0.3 mg/ml), chitosan in 1% acetic acid (0.3 mg/ml; pH 5), and $CaCl_2$ in aquabides (0.67 mg/ml). MCA-SGE was made by ionic gelation method by gradually mixing each component and homogenizing using a magnetic stirrer, ultra turax and sonification process. The formed MCA-SGE was stored at 4°C (Natrajan et al. 2015).

Characterisation of MCA-SGE

a. Particle Size Analyser (PSA)

The average particle size, polydispersity index (PDI), and zeta potential (ZP) were characterized using PSA Nano-Zetasizer Ver. 7.01 (Malvern Instruments Ltd.) with Dynamic Light Scattering (DLS) technique (Sorasitthiyanukarn et al. 2018). MCA-SGE samples that have been diluted with deionized water are placed in a cuvette for analysis at 25°C (Natrajan et al. 2015; Filho et al. 2019).

b. Scanning Electron Microscopy (SEM)

MCA-SGE which has been spray dried was used for this analysis. 0.5 g of MCA-SGE powder was then imaged with Scanning Electron Microscopy (SEM) (Natrajan et al. 2015).

c. Fourier Transform Infrared Spectroscopy (FTIR)

The FTIR test was carried out using a modified research method by Praseptiangga et al. (2020), 2 mg of samples were taken and tested with an IR spectrophotometer Shimadzu IR Spirit–T analysed with Shimadzu LabSolutions IR, the test was carried out with a scan number of 10, and a resolution of 4 cm^{-1}.

MCA-SGE Biological Test

a. Antioxidant Activity Test

Antioxidant activity test can with DPPH (1,1-diphenyl-2-picrylhydrazyl) test. Testing of antioxidant activity using the procedure of (Rajasree et al. 2021), with modifications. DPPH solution (50 mM) was mixed in samples (5:1) of various concentrations (including 3000 ppm, 6000 ppm, 12000 ppm, 24000 ppm), and 1 ml of DPPH solution (50 µM) for control. Then it was incubated for 30 minutes at room temperature in the dark, absorbance was measured in a spectrophotometer at 517 nm, and the results are used to calculate the percentage of antioxidants (%) through the formula in equation (1).

$$\% \ Antioxidants = \frac{A0 - A1}{A0} \ x \ 100 \qquad (1)$$

Information:

A0 = control absorbance

A1 = sample absorbance

In-vitro Kinetic Release Test

A total of 3 ml of MCA-SGE solution in PBS was put into a cellophane bag and immersed in 25 ml of PBS solution containing 20% ethanol at pH 1.5 as the release medium. The study was started by gently stirring at 37°C for a time of 4 hours. Then HPLC was analysed to determine the levels of the active compounds allicin and alliin. The percentage of kinetic release was calculated using the formula in equation (2).

$$Kinetic\ Release\ Percentage\ (\%) = \frac{levels\ of\ active\ compounds\ after}{levels\ of\ active\ compounds\ before} \times 100 \qquad (2)$$

RESULTS AND DISCUSSION

Characterisation of MCA-SGE

Based on the results of the MCA-SGE Z-Average characterization, the particle size is 439.0 ± 1.9 nm and SGE is 350.67 ± 2.14 nm (Table 1). Z-Average uses the principle of dynamic light scattering, so it has a larger average particle diameter size than measurements with a regular microscope. Particle size is caused by the concentration of the constituent components of the nanoparticle (Chopra et al. 2012). The addition of chitosan and $CaCl_2$ increases the average particle size (Yousefi et al. 2020). According to Fei et al. (2015) the pH factor and the ability of kinetic reactions between material particles also affect the size in the formation of microencapsulation. The ionic interaction between chitosan and alginate forms an electrostatic bond which also gives rise to an increase in particle size because it includes a polyelectrolyte membrane on the surface of the microcapsule. Microcapsule particle size > 200 µm has a higher control release (Dima et al. 2013).

Table 1. Characterisation of PSA MCA- SGE.

Characterisation of PSA	MCA-SGE	SGE
Particle size/*Z-average* (nm)	439.0 ± 1.9	350.67 ± 2.14
Polydispersity Index	0.579 ± 0.046	0.75 ± 0.01
Zeta Potential (mV)	-15.4 ± 0.3	not analysed

The *Z-Average* value is used to determine the average size of MCA-SGE and SGE particles, while the PDI value of MCA-SGE and SGE is used to determine the homogeneity distribution of particles. The PDI value is used to determine the distribution of particle homogeneity. A good PDI value or indicating homogeneous particles is less than 0.500 or close to 0 (Aleksandra Zielińska et al. 2020). A graph of the MCA-SGE and SGE particle size distribution can be seen in Figure 1.

The results of the characterisation of PDI MCA-SGE are 0.579 ± 0.046 and SGE are 0.75 ± 0.01 (Table 1). A PDI value close to 0 indicates that the distribution of particle homogeneity is high (mono dispersity), while a higher PDI value (close to 1) indicates that the particles are widely distributed (polydispersity) or heterogeneous (Danaei et al. 2018). Research by Wang et al. (2016) reported that the PDI value of MCA ranged from 0.340 ± 0.040 so the particles were said to be homogeneous. The PDI value of MCA-SGE and SGE was higher than 0.500 so both of them were categorised as heterogeneous because most of the MCA-SGE and SGE particles were not formed, and the resulting sizes varied. The high value of PDI also occurs due to weak ionic interactions between the constituent components which result in particle aggregation or clumping (Loquercio et al. 2015).

The zeta potential value indicates the stability of a microencapsulated suspension. The zeta potential value of MCA-SGE is -15.4 ± 0.4 mV (Table 1). The zeta potential value of microencapsulation is affected

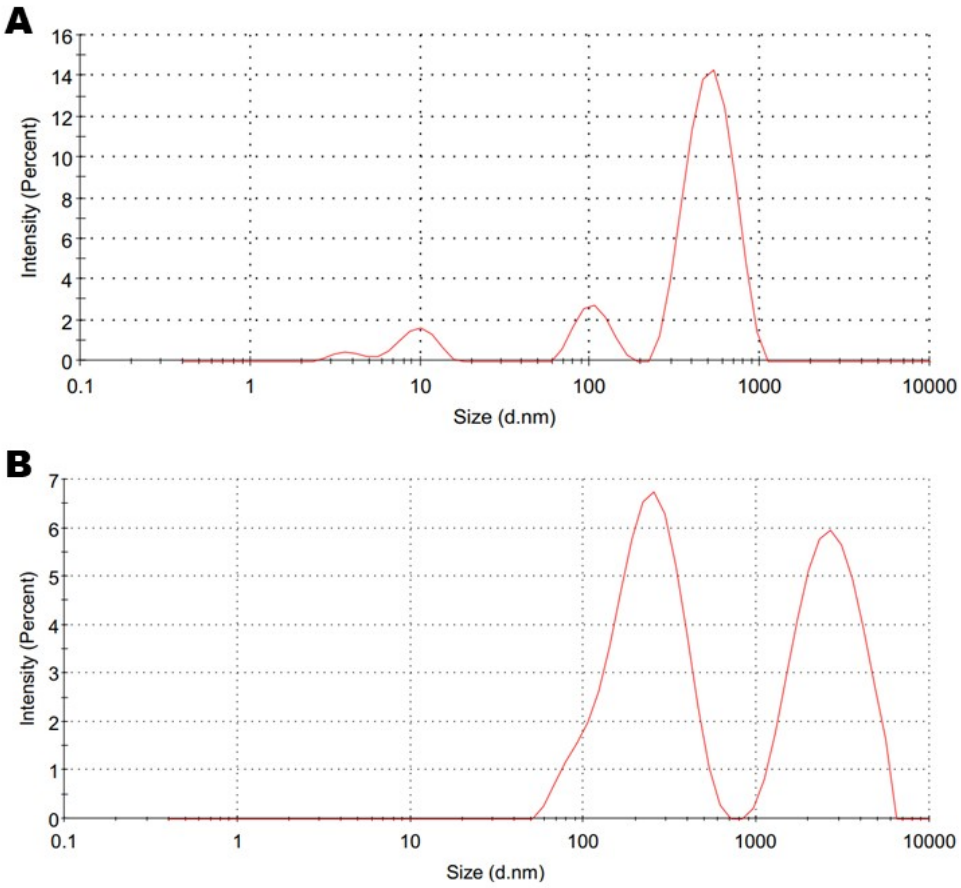

Figure 1. Profile of particle size distribution by intensity. (A) Particle size distribution of MCA-SGE. (B) Particle size distribution SGE.

by surface chemistry, particle concentration, size of particle, pH of the medium, temperature, solvent, and ionic strength (dos Santos et al. 2015; Mudalige et al. 2018). Zeta potential is important to know because it can affect the stability of colloidal systems, the interaction of nanoparticles with other charged molecules, and the efficiency of drug delivery (Kyzioł et al. 2017). The zeta potential value of MCA-SGE (Table 1) is in the range of ±10.0 mV to ±30.0 mV, where the particles are classified as less stable (Aziz et al. 2013). The colloidal system will tend to agglomerate (aggregate) because the repulsion between the particles is low (Zhou et al. 2018). This negative MCA-SGE zeta potential could be due to the high concentration of alginate (Krisanti et al. 2017). This is following (Wang et al. 2016) who reported that a higher alginate ratio resulted in more anions in the system or in other words the amount of $NH3^+$ chitosan charge was lower than the COO-alginate charge, thus causing the zeta potential value of the system to be less positive. Microparticles are said to have good mucoadhesive if they have a zeta potential value between 20-50 mV (Krisanti et al. 2017).

Scanning Electron Microscopy (SEM)

The results of the morphological characterization of MCA-SGE using SEM are shown in Figure 2A shows MCA-SGE (100x) which is shaped like a lump of agglomerated particles. Figure 2B shows the MCA-SGE (1000 x) particles of non-uniform size. Figure 2C (10,000x) shows the spherical morphology of MCA-SGE with sizes in the micrometre range, i.e 0.422 – 0.719 μm, and has a smooth surface of microparticles.

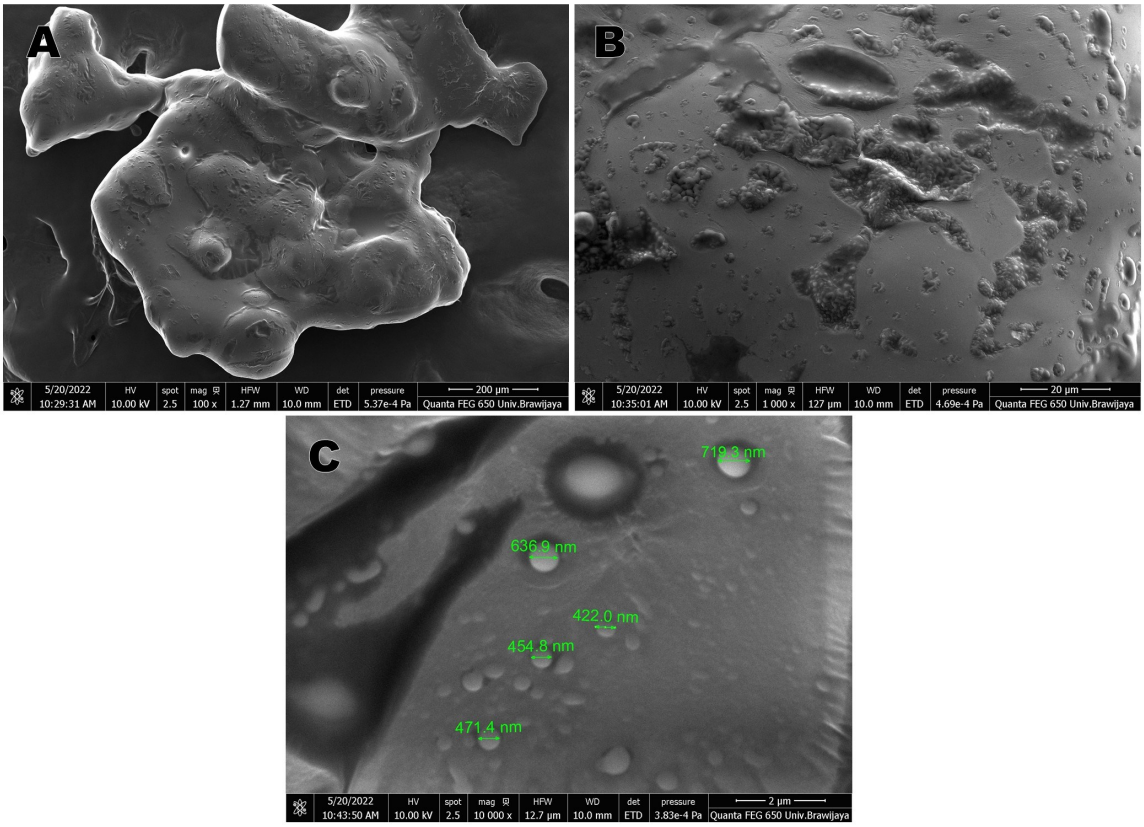

Figure 2. Morphology of MCA-EBT by scanning electron microscopy observation.

The morphology of MCA-SGE with a magnification of 100 x looks like a lump of agglomerated particles. This indicates that an agglomeration has formed. There are two causes of agglomeration, Brown agglomeration occurs when particles collide and stick together as a result of random Brownian motion, while gravitational agglomeration occurs when slowly settling particles are caught by faster settling particles, leading to the formation of lumps (Singer et al. 2018). The morphology of MCA-SGE with 10,000x magnification shows that the formed MCA-SGE particles are not uniform or different. The morphology of MCA-SGE with a magnification of 10,000x shows that MCA-SGE is round in shape with different sizes, which are in the range of 422 - 719 nm, and has a smooth surface of microparticles. Based on this size range, MCA-SGE is categorized as microparticles. Microparticles have particle sizes in the range of 1 to 1000 m (Lengyel et al. 2019b). MCA-SGE sizes in the range < 500 nm (422 nm, 455 nm, and 471 nm) are more easily absorbed by cells when in the body (Pudlarz & Szemraj 2018). The results of different sizes can be caused by particle aggregation (Michen et al. 2015). According to the research results of Natrajan et al. (2015), the morphology of the turmeric and lemongrass oil nanoencapsulation is also round but has an average size below 300 nm (Natrajan et al. 2015). Research by Buanasari et al. (2021) reported that plant extract microcapsules using chitosan were round with a smooth surface. However, sometimes capsules may also develop roughness on their surface during spray drying. And such imperfections are developed when the film formation process during drying of atomised droplets slow down. In a similar way, the internal morphology was analysed and it was observed that the micro- capsules obtained were hollow and the core material was stuck onto the surface, which is also a particle characteristic obtained using spray drying. Differences in wall material also affected the topography of the microcapsules formed (Choudhury et al. 2021).

Fourier Transform Infrared Spectroscopy (FTIR)

The infrared (IR) graph of SGE is presented in Figure 3, while the IR graph of MCA-SGE is presented in Figure 4. Functional groups that appear in the two samples include amine and hydroxyl strains (N-H and O-H) indicated by the presence of absorption at 3344.47 cm^{-1} IR SGE. and absorption at 3343.04 cm^{-1} IR MCA-SGE; alkane group (C-H) indicated by the absorption at 2936.57 cm^{-1} IR SGE and absorption at 2928.01 cm^{-1} IR MCA-SGE; alkyl groups (C-H) were indicated by the presence of absorption at 1454.74 cm^{-1} IR SGE and IR MCA-SGE; aromatic amine group (C-N) was indicated by the absorption at 1279.31 cm^{-1} IR SGE and absorption at 1283.59 cm^{-1} IR MCA-SGE; cyclohexane compound (C-H) was indicated by the absorption at 934.17 cm^{-1} IR SGE and absorption at 935.59 cm^{-1} IR MCA-SGE; aromatic compounds (C-H) were indicated by the absorption at 818.65 cm^{-1} IR SGE and absorption at 821.50 cm^{-1} IR MCA-SGE; disulfide group (C-S) was indicated by the absorption at 599.01 cm^{-1} IR SGE and absorption at 600.44 cm^{-1} IR MCA-SGE. A number of other uptakes showing different functional groups at IR SGE and IR MCA-SGE are presented in Table 2 and Table 3.

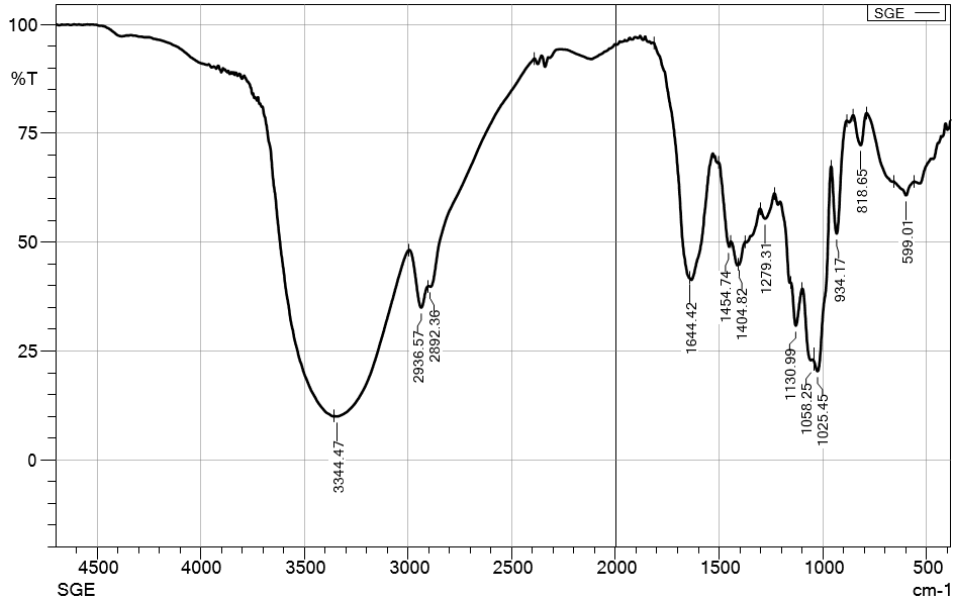

Figure 3. IR Graph Profil of SGE.

Table 2. List of IR SGE Absorption and Functional Groups.

Absorbance (cm^{-1})	Bond Type	Functional groups	Reference
599.01	C–S	Disulfide	
818.65	C–H 1,4 (para)	Aromatic compounds	
934.17	C–H	cyclohexane	
1025.45	C–F	Aromatic fluoro compounds	(Nandiyanto et al. 2019)
1058.25	C–O	Ether	
1130.99	C–N	Amine	
1279.31	C–N	Aromatic amine	
1404.82	O–H	Carboxylic acid	(Merck 2022)
1454.74	C–H	Alkyl	
1644.42	N–H	Amine	(Nandiyanto et al. 2019)
2892.36	C–H	Metin	
2936.57	C–H	Alkanes	(Merck 2022)
3344.47	N–H & O–H	Amines and Hydroxyl	(Nandiyanto et al. 2019; Merck 2022)

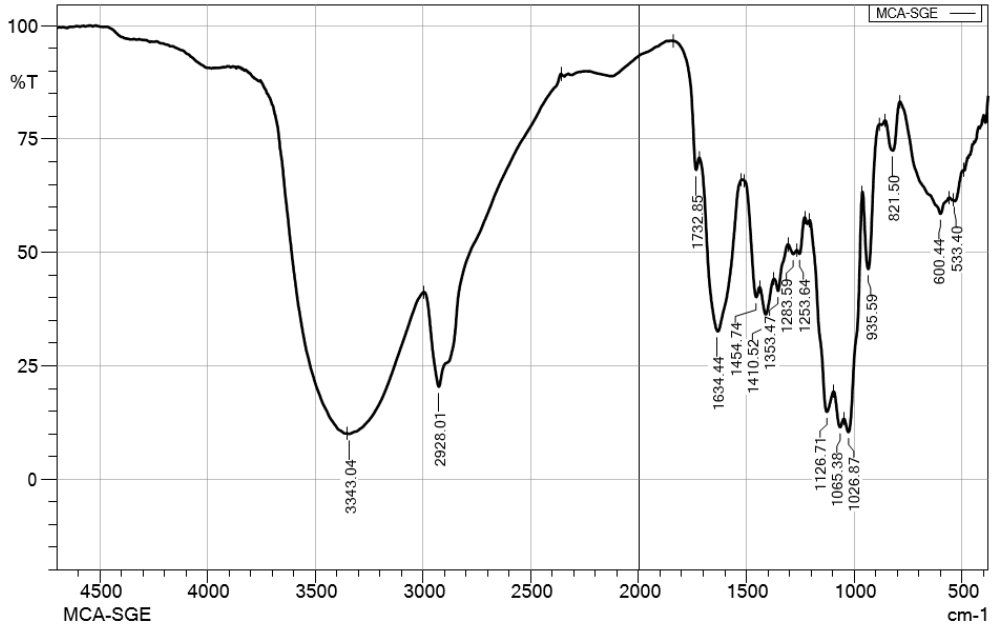

Figure 4. IR Graph Profile of MCA-SGE.

Table 3. List of MCA-SGE IR Absorption and Functional Groups.

Absorbance (cm^{-1})	Bond Type	Functional groups	Reference
533.40	C–I	Aliphatic iodo compounds	(Nandiyanto et al. 2019)
600.44	C–I	Aliphatic iodo compounds	
821.50	C–H 1,4 (para)	Aromatic compounds	
935.59	C–H	cyclohexane	(Merck 2022)
1026.87	C–N	Amine	
1065.38	C–N	Amine	
1126.71	C–O	Alcohol	(Nandiyanto et al. 2019)
1253.64	–O	Aromatic ether	
1283. 59	C–N	Aromatic amine	
1353.47	O–H	Alcohol	(Merck 2022)
1410.52	$–COO^-$	Carboxylate	(Nandiyanto et al. 2019)
1454.74	C–H	Alkyl	
1634.44	C=O	Amide I	(Nandiyanto et al. 2019; Merck 2022)
1732.85	C=O	Esther	(Merck 2022)
2928.01	C–H	Alkanes	(Nandiyanto et al. 2019; Merck 2022)
3343.04	N–H & O–H	Amine	

Absorption of 3344.47 cm^{-1}, 1644.42 cm^{-1}, 1279.31 cm^{-1}, and 1130.99 cm^{-1} on SGE indicated an amine compound. The number of amine groups that are read on SGE indicates the presence of alliin and allicin content (Borlinghaus et al. 2014). The IR SGE graph also shows the presence of carbonyl, carboxylate and aromatic compounds (Table 2). Carbonyl compounds, carboxylate compounds and aromatic compounds were visible in the FTIR results of garlic methanol extract (Divya et al. 2017).

The MCA-SGE graph shows some additional absorptions that provide information on the functional groups of the encapsulated material. Chitosan gives rise to absorption at 1634.44 cm^{-1} which is the am-

ide I functional group (Filho et al. 2019). Another material that gives rise to absorption at 1732.85 cm^{-1} is an ester group that can be found in sodium alginate (Szabó et al. 2020). Some absorptions at 1065.38 cm^{-1}, 1410.52 cm^{-1}, 1634.44 cm^{-1}, and 3343.04 cm^{-1} respectively were amine (C-N), carboxylate (COO-), amide (N-H) and amine and hydroxyl (N-H) strains. and O-H). These four functional groups appear when the combination of chitosan-alginate material is used in encapsulation (Ahmad et al. 2022). Other absorptions such as at 1025.45 cm^{-1} (aliphatic compound) IR SGE shifted at 1026.87 cm^{-1} at IR MCA-SGE. Absorption at 1130.99 cm^{-1} (amine) IR SGE shifted at 1126.71 cm^{-1} at IR MCA-SGE. The absorption at 1279.31 (aromatic amine) IR SGE shifted at 1283.59 cm^{-1} IR MCA-SGE. The absorption at 1454.74 cm^{-1} (alkyl) IR SGE shifted at 1454.74 cm^{-1} IR MCA-SGE. The shift in the absorption value that occurs indicates an interaction in the form of an electrostatic force between SGE and the encapsulation constituent materials.

Antioxidant Activity

Antioxidants play an important role in protecting the body from the influence of free radicals and oxidative damage, so the presence of antioxidants in the body is important (Kurnia et al. 2021) Antioxidants react with DPPH through very fast electron transfer and with slow transfer of hydrogen atoms, this reaction causes antioxidant compounds to inhibit the action of free radicals (Schaich et al. 2015; Abbaspour-Gilandeh et al. 2021).

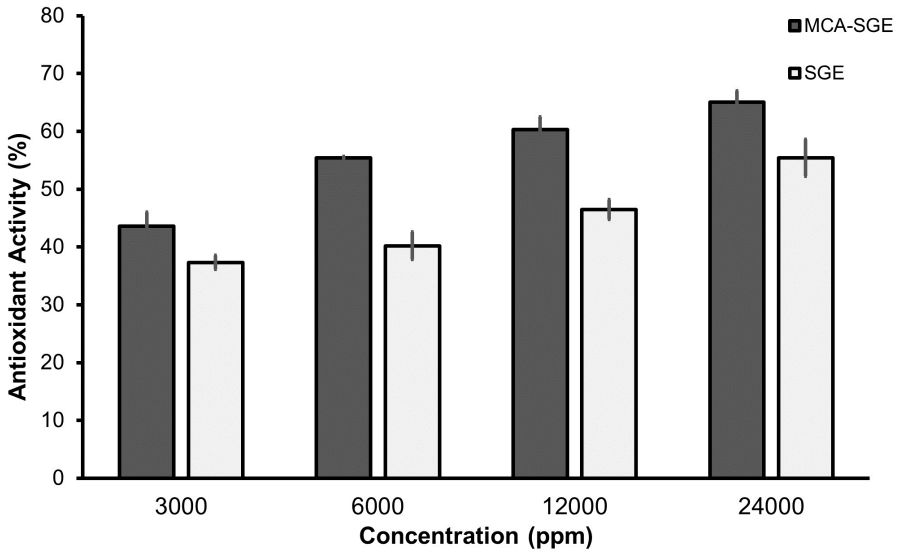

Figure 5. Antioxidant Activity of SGE and MCA-SGE.

Data from the DPPH test results showed (Figure 5) there was an increase in the percentage of antioxidants with an increase in the concentration level of SGE and MCA-SGE. MCA-SGE tends to have higher antioxidants than SGE. The higher antioxidants of MCA-SGE compared to SGE may be due to additional antioxidant components from the ingredients used in microencapsulated formulations. It is mentioned that alginate oligosaccharides have antioxidant activity (Zhang et al. 2020) In addition, chitosan also has radical damping activity from the hydroxyl group and the amino group (Avelelas et al. 2019) This result is supported by the previous research that the encapsulation of garlic oil with chitosan polymer increases antioxidant activity (Amiri et al. 2021). Other studies also describe a similar thing that one of the main aspects of microencap-

sulation is to improve bioavailability of food antioxidants (Ozkan et al. 2019). Microencapsulation protects bioactive compounds (mainly antioxidant compounds) effectively against destructive environmental conditions, in addition to providing physical stability, improved bio-accessibility, as well as controlled release over time (Mohammadalinejhad & Kurek 2021). High concentration will be more effective in becoming a better pro-oxidant (Bagheri et al. 2016)

Release Kinetic (RK) in vitro

The kinetic release test results of *allicin* and *alliin* compounds in single garlic extract chitosan-alginate microencapsulation (MCA-SGE) were carried out in the gastric environment (pH 1.5). The significance value in the T-paired Test between the levels of allicin and alliin compounds in SGE and MCA-SGE shows a signification of < 0.05 so that there is an average difference between the levels of *allicin* and *alliin* compounds SGE and MCA-SGE before the kinetic release test. Decreasing of active compounds after kinetic release tests also occur in MCA-SGE (Table 4).

The percentage of kinetic release of allicin and alliin compounds in SGE is greater with a percentage value of 86% than that of MCA-SGE which is in the range of values of 64.58% in *allicin* and 58.81 % in *alliin*. Microencapsulation has the potential to reduce the release of a single garlic active compound from the low pH of the gastric gastrointestinal fluid. It is reported that chitosan and alginate used can control the release of encapsulated compounds (Park et al. 2022; Waqas et al. 2022). Controlled drug delivery systems have been developed to improve the next staging of the drug in the body with two main purposes, to reduce the number of single doses per day improving patient compliance of treatments and to decrease the fluctuations of plasma levels, in order to obtain better therapeutic efficacy and lower toxicity (Saha & Das 2015). Previous research showed that during a span of 4 hours, when it was at pH 1.5 the kinetic release results of turmeric oil and citronella oil encapsulated with chitosan-alginate were about 35% and 5%, respectively (Natrajan et al. 2015).

The release of the drug has a sensitivity to pH, alginate is less easily soluble in low pH than chitosan. The interaction of encapsulated materials at a low pH will further help the release of active compounds when exposed to blood pH (pH 7.4). This causes more bioactive ingredients to be absorbed into the blood system and later the bioactive ingredients are transported in the circulatory system (Patel et al. 2013).

Table 4. Results of In-vitro Kinetic Release Test of SGE and MCA-SGE.

Sample	Pre-RK levels (µg/ml)		Levels after RK (µg/ml)		Percentage Release Kinetic (%)	
	Allicin	***Alliin***	***Allicin***	***Alliin***	***Allicin***	***Alliin***
SGE	52090.57 ± 4025.62	31080.76 ± 2403.78	44872.23 ± 5486.90	26770.54 ± 3276.35	86.16 ± 8.58	86.15 ± 8.59
MCA-SGE	102150.72 ± 12067.78	64868.34 ± 7665.89	62215.23 ± 5598.78	35973.41 ± 3239.49	64.58 ± 4.07	58.81 ± 3.71

CONCLUSIONS

MCA-SGE is efficient as a drug delivery agent for SGE based on characterisation (PSA, SEM, and FTIR analysis), antioxidant activity, and kinetic release. The MCA-SGE based on PSA analysis were successfully prepared and showed good characteristics in range micrometer. FTIR study reported a shift in absorption and addition of SGE functional groups after encapsulation. The results of the antioxidant activity test showed that the antioxidant activity of MCA-SGE was higher than SGE and could be used as a drug delivery system with controlled release.

AUTHOR CONTRIBUTION

S.R.L., A.G., S.I.M. and S. designed the research and supervised the process. A.N.R, D.N.A, I.N.M, and N.D.R prepared the MCA-SGE formulation, and collected the data. N.P., D.S.M and A.R.E.B collected, to analyse the data and prepared the manuscript.

ACKNOWLEDGMENTS

This research was funded by Directorate of Research, Technology, and Community Service, The Ministry of Education, Culture, Research, and Technology Republic Indonesia, the Fundamental Research Scheme – National Competition Research with contract number 20.06.38/UN32.20.1/LT/2023.

CONFLICT OF INTEREST

The authors declare that they do not have a conflict of interest.

REFERENCES

Abbaspour-Gilandeh, Y. et al., 2021. Combined hot air, microwave, and infrared drying of hawthorn fruit: Effects of ultrasonic pretreatment on drying time, energy, qualitative, and bioactive compounds' properties. *Foods*, 10(5). doi: 10.3390/foods10051006.

Abdel-Gawad, M. et al., 2018. in Vitro Antioxidant, Total Phenolic and Flavonoid Contents of Six Allium Species Growing in Egypt. *Journal of Microbiology, Biotechnology and Food Sciences*, 8(2), pp.343–346.

Ahmad, R.M. et al., 2022. Preparation and Characterization of Blank and Nerolidol-Loaded Chitosan–Alginate Nanoparticles. *Nanomaterials*, 12(7), 1183. doi: 10.3390/nano12071183

Akhter, M.H. et al., 2022. Drug Delivery Challenges and Current Progress in Nanocarrier-Based Ocular Therapeutic System. *Gels*, 8(2). doi: 10.3390/gels8020082.

Aleksandra Zielińska et al., 2020. Polymeric Nanoparticles: Production, Characterization, Toxicology and Ecotoxicology. *Molecules*, 25, p.3731. doi: 10.3390/molecules25163731

Alencar, D.D. de O. et al., 2022. Microencapsulation of Cymbopogon citratus D.C. Stapf Essential Oil with Spray Drying: Development, Characterization, and Antioxidant and Antibacterial Activities. *Foods*, 11(8). doi: 10.3390/foods11081111.

Amiri, N. et al., 2021. Nanoencapsulation (in vitro and in vivo) as an efficient technology to boost the potential of garlic essential oil as alternatives for antibiotics in broiler nutrition. *Animal*, 15(1), 100022. doi: 10.1016/j.animal.2020.100022.

Avelelas, F. et al., 2019. Antifungal and antioxidant properties of chitosan polymers obtained from nontraditional Polybius henslowii sources. *Marine Drugs*, 17(4), pp.1–15. doi: 10.3390/md17040239.

Aziz, S.A.A. et al., 2013. Effect of Zeta Potential of Stanum Oxide (SnO2) on Electrophoretic Deposition (EPD) on Porous Alumina. *Advanced Materials Research*, 795, pp.334–337. doi: 10.4028/www.scientific.net/AMR.795.334.

Bagheri, R. et al., 2016. Comparing the effect of encapsulated and unencapsulated fennel extracts on the shelf life of minced common kilka (Clupeonella cultriventris caspia) and Pseudomonas aeruginosa inoculated in the mince. *Food Science and Nutrition*, 4(2), pp.216–222. doi: 10.1002/fsn3.275.

Baltrusch, K.L. et al., 2022. Spray-drying microencapsulation of tea extracts using green starch, alginate or carrageenan as carrier materials. *International Journal of Biological Macromolecules*, 203, pp.417–429. doi: 10.1016/j.ijbiomac.2022.01.129.

Bhatwalkar, S.B. et al., 2021. Antibacterial Properties of Organosulfur Compounds of Garlic (Allium sativum). *Frontiers in Microbiology*, 12 (July), pp.1–20. doi: 10.3389/fmicb.2021.613077.

Borlinghaus, J. et al., 2014. Allicin: chemistry and biological properties. *Molecules (Basel, Switzerland)*, 19(8), pp.12591–12618. doi: 10.3390/molecules190812591.

Buanasari, Sugiyo, W. & Rustaman, H., 2021. Preparation and evaluation of plant extract microcapsules using Chitosan. *IOP Conference Series: Earth and Environmental Science*, 755(1). doi: 10.1088/1755-1315/755/1/012063.

Chopra, M. et al., 2012. Synthesis and Optimization of Streptomycin Loaded Chitosan-Alginate Nanoparticles. *International Journal of Scientific & Technology Research*, 1(10), pp.31–34.

Choudhury, N., Meghwal, M. & Das, K., 2021. Microencapsulation: An overview on concepts, methods, properties and applications in foods. *Food Frontiers*, 2(4), pp.426–442. doi: 10.1002/fft2.94.

Danaei, M. et al., 2018. Impact of Particle Size and Polydispersity Index on the Clinical Applications of Lipidic Nanocarrier Systems. *Pharmaceutics*, 10(2), 57. doi: 10.3390/pharmaceutics10020057.

Dima, C. et al., 2013. Microencapsulation of coriander oil using complex coacervation method. *Scientific Study and Research: Chemistry and Chemical Engineering, Biotechnology, Food Industry*, 14(3), pp.155–162.

Divya, B. et al., 2017. A Study on Phytochemicals, Functional Groups and Mineral Composition of Allium sativum (Garlic) Cloves. doi: 10.22159/ijcpr.2017v9i3.18888.

Fei, X. et al., 2015. Microencapsulation mechanism and size control of fragrance microcapsules with melamine resin shell. *Colloids and Surfaces A: Physicochemical and Engineering Aspects*, 469, pp.300–306. doi: 10.1016/j.colsurfa.2015.01.033.

Filho, J.C.P. et al., 2019. Design of chitosan-alginate core-shell nanoparticules loaded with anacardic acid and cardol for drug delivery. *Polimeros*, 29(4), pp.1–10. doi: 10.1590/0104-1428.08118.

Katuwavila, N.P. et al., 2016. Chitosan-Alginate Nanoparticle System Efficiently Delivers Doxorubicin to MCF-7 Cells. *Journal of Nanomaterials*, 2016. doi: 10.1155/2016/3178904.

Krisanti, E., Aryani, S.D. & Mulia, K., 2017. Effect of chitosan molecular weight and composition on mucoadhesive properties of mangostin-loaded chitosan-alginate microparticles. *AIP Conference Proceedings*, 1817. doi: 10.1063/1.4976766.

Kurnia, D. et al., 2021. Antioxidant properties and structure-antioxidant activity relationship of allium species leaves. *Molecules*, 26(23), pp.1–28. doi: 10.3390/molecules26237175.

Kyriakoudi, A. et al., 2021. Innovative delivery systems loaded with plant bioactive ingredients: Formulation approaches and applications. *Plants*, 10(6), pp.1–56. doi: 10.3390/plants10061238.

Kyzioł, A. et al., 2017. Preparation and characterization of alginate/chitosan formulations for ciprofloxacin-controlled delivery. *Journal of Biomaterials Applications*, 32(2), pp.162–174. doi: 10.1177/0885328217714352.

Lengyel, M. et al., 2019a. Microparticles, microspheres, and microcapsules for advanced drug delivery. *Scientia Pharmaceutica*, 87(3). doi: 10.3390/scipharm87030020.

Lengyel, M. et al., 2019b. Microparticles, Microspheres, and Microcapsules for Advanced Drug Delivery. *Scientia Pharmaceutica*, 87(3), pp.1–31.

Lestari, S.R. & Rifa'i, M., 2018. Regulatory T cells and anti-inflammatory cytokine profile of mice fed a high-fat diet after single-bulb garlic (Allium sativum L.) oil treatment. *Tropical Journal of Pharmaceutical Research*, 17(11), pp.2157–2162. doi: 10.4314/tjpr.v17i11.7.

Lestari, S.R. et al., 2020. Single Garlic Oil Modulates T Cells Activation and Proinflammatory Cytokine in Mice with High Fat Diet. *Journal of Ayurveda and Integrative Medicine*, 11(4), pp.414–420. doi: 10.1016/j.jaim.2020.06.009.

Lestari, S.R. et al., 2021. Self-nanoemulsifying drug delivery system (SNEEDS) for improved bioavailability of active compound on single clove garlic: Optimization of PEG 400 and glycerol as co-surfactant. *AIP Conference Proceedings*, 2353. doi: 10.1063/5.0052638.

Loquercio, A. et al., 2015. Preparation of Chitosan-Alginate Nanoparticles for Trans-cinnamaldehyde Entrapment. *Journal of Food Science*, 80(10), pp.N2305–N2315. doi: 10.1111/1750-3841.12997.

Machado, N.D. et al., 2021. Preservation of the antioxidant capacity of resveratrol via encapsulation in niosomes. *Foods*, 10(5), pp.1–12. doi: 10.3390/foods10050988.

Merck, 2022. IR Spectrum Table & Chart.

Michen, B. et al., 2015. Avoiding drying-artifacts in transmission electron microscopy: Characterizing the size and colloidal state of nanoparticles. *Scientific Reports*, 5. doi: 10.1038/srep09793.

Mohammadalinejhad, S. & Kurek, M.A., 2021. Applsci-11-03936.Pdf. *Applied Sciences*.

Mudalige, T. et al., 2018. Characterization of Nanomaterials: Tools and Challenges.In *Micro and Nano Technologies, Nanomaterials for Food Applications*. Elsevier Inc. pp.313–353. doi: 10.1016/B978-0-12-814130-4.00011-7.

Nandiyanto, A.B.D., Oktiani, R. & Ragadhita, R., 2019. How to read and interpret ftir spectroscope of organic material. *Indonesian Journal of Science and Technology*, 4(1), pp.97–118. doi: 10.17509/ijost.v4i1.15806.

Natrajan, D. et al., 2015. Formulation of essential oil-loaded chitosan-alginate nanocapsules. *Journal of Food and Drug Analysis*, 23(3), pp.560–568. doi: 10.1016/j.jfda.2015.01.001.

Ozkan, G. et al., 2019. A review of microencapsulation methods for food antioxidants: Principles, advantages, drawbacks and applications. *Food Chemistry*, 272(August 2018), pp.494–506. doi: 10.1016/j.foodchem.2018.07.205.

Park, K.H. et al., 2022. Controlled Drug Release Using Chitosan-Alginate-Gentamicin Multi-Component Beads. , pp.1–13.

Pateiro, M. et al., 2021. Nanoencapsulation of promising bioactive compounds to improve their absorption, stability, functionality and the appearance of the final food products. *Molecules*, 26(6). doi: 10.3390/molecules26061547.

Patel, B.K., Parikh, R.H. & Aboti, P.S., 2013. Development of Oral Sustained Release Rifampicin Loaded Chitosan Nanoparticles by Design of Experiment. *Journal of Drug Delivery*, 2013, pp.1–10. doi: 10.1155/2013/370938.

Pedroso-Santana, S. & Fleitas-Salazar, N., 2020. Ionotropic gelation method in the synthesis of nanoparticles/microparticles for biomedical purposes. *Polymer International*, 69(5), pp.443–447. doi: 10.1002/pi.5970.

Praseptiangga, D. et al., 2021. Preparation and FTIR spectroscopic studies of SiO2-ZnO nanoparticles suspension for the development of carrageenan-based bio-nanocomposite film. *AIP Conf. Proc.*, 2219, 100005. doi: 10.1063/5.0003434

Pudlarz, A. & Szemraj, J., 2018. Nanoparticles as carriers of proteins, peptides and other therapeutic molecules. *Open Life Sciences*, 13(1), pp.285–298. doi: 10.1515/biol-2018-0035.

Qadariah, N., Lestari, S.R. & Rohman, F., 2020. Single Bulb Garlic (*Allium Sativum*) Extract Improve Sperm Quality in Hyperlipidemia Male Mice Model. *Jurnal Kedokteran Hewan - Indonesian Journal of Veterinary Sciences*, 14(1), pp.7–11. doi: 10.21157/j.ked.hewan.v14i1.13562.

Rajasree, R.S. et al., 2021. An evaluation of the antioxidant activity of a methanolic extract of cucumis melo l. Fruit (f1 hybrid). *Separations*, 8(8), pp.1–15. doi: 10.3390/separations8080123.

Saha, P. & Das, P.S., 2015. Advances in Controlled Release Technology in Pharaceuticals: A Review. *World journal of pharmacy and pharmaceutical sciences*, 6(9), pp.2070–2084. doi: 10.20959/wjpps20179-10194.

dos Santos, P.P. et al., 2015. Development of lycopene-loaded lipid-core nanocapsules: physicochemical characterization and stability study. *Journal of Nanoparticle Research*, 17(2). doi: 10.1007/s11051-015-2917-5.

Sasi, M. et al., 2021. Garlic (Allium sativum L.) bioactives and its role in alleviating oral pathologies. *Antioxidants*, 10(11). doi: 10.3390/antiox10111847.

Schaich, K.M., Tian, X. & Xie, J., 2015. Hurdles and pitfalls in measuring antioxidant efficacy: A critical evaluation of ABTS, DPPH, and ORAC assays. *Journal of Functional Foods*, 14, pp.111–125. doi: 10.1016/j.jff.2015.01.043.

Shang, A. et al., 2019. Bioactive compounds and biological functions of garlic (allium sativum L.). *Foods*, 8(7), pp.1–31. doi: 10.3390/foods8070246.

Singer, A. et al., 2018. Nanoscale Drug-Delivery Systems: In Vitro and In Vivo Characterization. *Nanocarriers for Drug Delivery: Nanoscience and Nanotechnology in Drug Delivery*, pp.395–419. doi: 10.1016/B978-0-12-814033-8.00013-8.

Sorasitthiyanukarn, F.N. et al., 2018. Chitosan/alginate nanoparticles as a promising approach for oral delivery of curcumin diglutaric acid for cancer treatment. *Materials Science and Engineering C*, 93(July), pp.178–190. doi: 10.1016/j.msec.2018.07.069.

Szabó, L., Gerber-Lemaire, S. & Wandrey, C., 2020. Strategies to functionalize the anionic biopolymer na-alginate without restricting its polyelectrolyte properties. *Polymers*, 12(4). doi: 10.3390/POLYM12040919.

Szychowski, K.A. et al., 2018. Characterization of Active Compounds of Different Garlic (Allium sativum l.) Cultivars. *Polish Journal of Food and Nutrition Sciences*, 68(1), pp.73–81. doi: 10.1515/pjfns-2017-0005.

Tao, Q. et al., 2021. Ionic and enzymatic multiple-crosslinked nanogels for drug delivery. *Polymers*, 13(20). doi: 10.3390/polym13203565.

Wang, F. et al., 2016. Effective method of chitosan-coated alginate nanoparticles for target drug delivery applications. *Journal of Biomaterials Applications*, 31(1), pp.3–12. doi: 10.1177/0885328216648478.

Waqas, M.K. et al., 2022. Alginate-coated chitosan nanoparticles for pH-dependent release of tamoxifen citrate. *Journal of Experimental Nanoscience*, 17(1), pp.522–534. doi: 10.1080/17458080.2022.2112919.

Yousefi, M. et al., 2020. Development, characterization and in vitro antioxidant activity of chitosan-coated alginate microcapsules entrapping Viola odorata Linn. extract. *International Journal of Biological Macromolecules*, 163, pp.44–54. doi: 10.1016/j.ijbiomac.2020.06.250.

Zhang, Y.H. et al., 2020. Characterization and Application of an Alginate Lyase, Aly1281 from Marine Bacterium Pseudoalteromonas carrageenovora ASY5. *Marine Drugs*, 18(2). doi: 10.3390/md18020095.

Zhou, P. et al., 2018. Loading BMP-2 on nanostructured hydroxyapatite microspheres for rapid bone regeneration. *International Journal of Nanomedicine*, 13, pp.4083–4092. doi: 10.2147/IJN.S158280.